Institute of Physics Publishing Journal of Physics: Conference Series **5** (2005) 105–114
doi:10.1088/1742-6596/5/1/010 International Workshop on Particle Multiplicity in Relativistic Heavy Ion Collisions

# Measuring charged particle multiplicity in ALICE

**Tiziano Virgili for the ALICE collaboration**[1]

Dipartimento di Scienze Fisiche "E.R. Caianiello" dell'Università and INFN, Salerno, Italy.

E-mail: tiziano.virgili@sa.infn.it

**Abstract.** The measure of the charged particle multiplicity in ALICE and the reconstruction of the pseudorapidity distribution will be mainly and most efficiently performed with the Silicon Pixel Detector for the central region, and with the Forward Multiplicity Detector at higher values of $\eta$, with a total coverage of almost 10 $\eta$-units.

## 1. Introduction

In high-energy hadron and heavy-ion collisions, the study of the global properties of the final state like the charged multiplicity plays a crucial role, since it allows us to determine the way in which the initial available center-of-mass energy is redistribuited in the accessible space phase. The dependence of multiplicity on the number of participants can also provide informations on the production mechanism. Moreover, the multiplicity of charged particles produced at central rapidity is related to the entropy density of the system formed in the collision [2] and to the initial energy density [3]. In the following the proposed methods of analysis and the main results determined by the simulation will be discussed.

## 2. Multiplicity and dN/d$\eta$ in the central region

The measure of the charged particle multiplicity and the reconstruction of the pseudorapidity distribution in the central region of $\eta$ is mainly and most efficiently performed with the two layers of silicon pixel detector.

Two different methods can be used:

(i) counting of the number of clusters $N_c$ for each layer;

(ii) counting of the number of "tracklets" $N_t$, where each tracklet is defined by the association of the clusters in the two layers. The association is done by considering a straight line to the primary vertex, assumed to be known [4], and within a fiducial window. This window is defined by the cuts on the longitudinal and radial residuals, i.e. the differences between the coordinates of the center of the cluster respect to the expectation from the straight line.

In both cases the pseudorapidity $\eta$ is evaluated by considering a straight line to the vertex.

### *2.1. The ALICE Silicon Pixel Detector*

The basic element of the ALICE SPD [5] is the ladder, consisting of a pixel detector matrix bonded to five front-end chips with fully independent readout. The detector matrix consists

[1] For the full list of the authors see ref. [1]

 

of $256 \times 160$ pixel cells, mostly measuring $50 \times 425$ $\mu$m$^2$, with a thickness of 150 $\mu$m. At the boundary between two front-end chips there are two columns of cells having dimensions of $50 \times 625$ $\mu$m$^2$. Four pixel ladders are aligned along their longer dimension to form a stave. The staves are arranged in space to form two cylindrical layers around the beam line. The first layer consists of 20 staves and has a radius of about 4 cm, the second one is formed by 40 staves, with a radius of about 7 cm. In layer 1 the staves are almost perpendicular to the radial direction, while in layer 2 they are tilted (turbo geometry) in order to ensure that no particle with momentum larger than 27 MeV/$c$ can go undetected through the openings among the staves.

With this geometry the acceptance regions are $|\eta| < 2$ for the inner layer, $|\eta| < 1.4$ for the outer layer. In total, the expected occupancy is lower than 1.5% and 0.4% for the two layers, considering a multiplicity limit of 8000 charged particles in the central unit of $\eta$.

*2.2. Simulation*

The simulation requires a complete description of the detector response, and an algorithm for cluster identification [6].

In principle a special running session with the L3 magnetic field off will offer the best configuration for this measure. For this reason most of the simulations are performed without magnetic field. Subsequently, the effect of the field was studied by a dedicated simulation, with different field values.

A sample of about 1000 events has been generated with HIJING 1.36 and tracked in the ALICE apparatus. The impact parameter was generated with a flat distribution in order to increase the statistics in the central class, then the appropriate weights have been introduced in order to reproduce a minimum bias distribution. A special sample of very low-multiplicity events was also generated by using a HIJING parametrization. As the acceptance and then the measured multiplicity depends on the vertex longitudinal position $z_v$, a scan on several $z_v$ values was also performed.

*2.3. Multiplicity measurement*

The correlation between the generated and the reconstructed multiplicity is shown in figure 1 for $z_v$=0. Here $dN/d\eta$ indicates the charged multiplicity in the central unit of $\eta$. The reconstructed $dN/d\eta$ is evaluated by counting the number of clusters $N_c$ in either layer 1 or layer 2 (top and middle plots), or by counting the number of tracklets (bottom). The statistical errors are smaller than the dimension of the symbols in figure. The hit multiplicities $N_h$ produced by the primary particles are also reported, where a hit is defined by the crossing of a particle on a layer through its sensitive volume. There is almost no difference between $N_c$ and $N_h$ in layer 1 (upper plot), both being slightly lower than the ideal value (the straight line, corresponding to the diagonal) due to small geometrical losses and cluster merging at high multiplicity. On the contrary, $N_c$ is enhanced in layer 2 by the secondaries produced in the inner layer and by the double hits of the tracks due to the "turbo geometry" (central plot).

The situation for the tracklets is close to that of layer 1, but at high multiplicity some inefficiency is visible (bottom plot). In principle the second method (tracklets) should be cleaner, allowing for background rejection (noise, secondary particles), but the association efficiency decreases as a function of the multiplicity. On the contrary, the first method is more reliable at high multiplicity, as the statistical fluctuations become negligible. However, the level of background can have a large influence on the cluster number.

In figure 2 the reconstruction of the multiplicity distribution for the mimum bias sample is compared with the generated one. A small difference is seen at the largest multiplicity, as already shown in figure 1. At high multiplicity the statistical fluctuations are completely negligible compared with the systematic effects (see figure 1). These effects are accounted for by the simulation, the main source being the production of background secondaries.

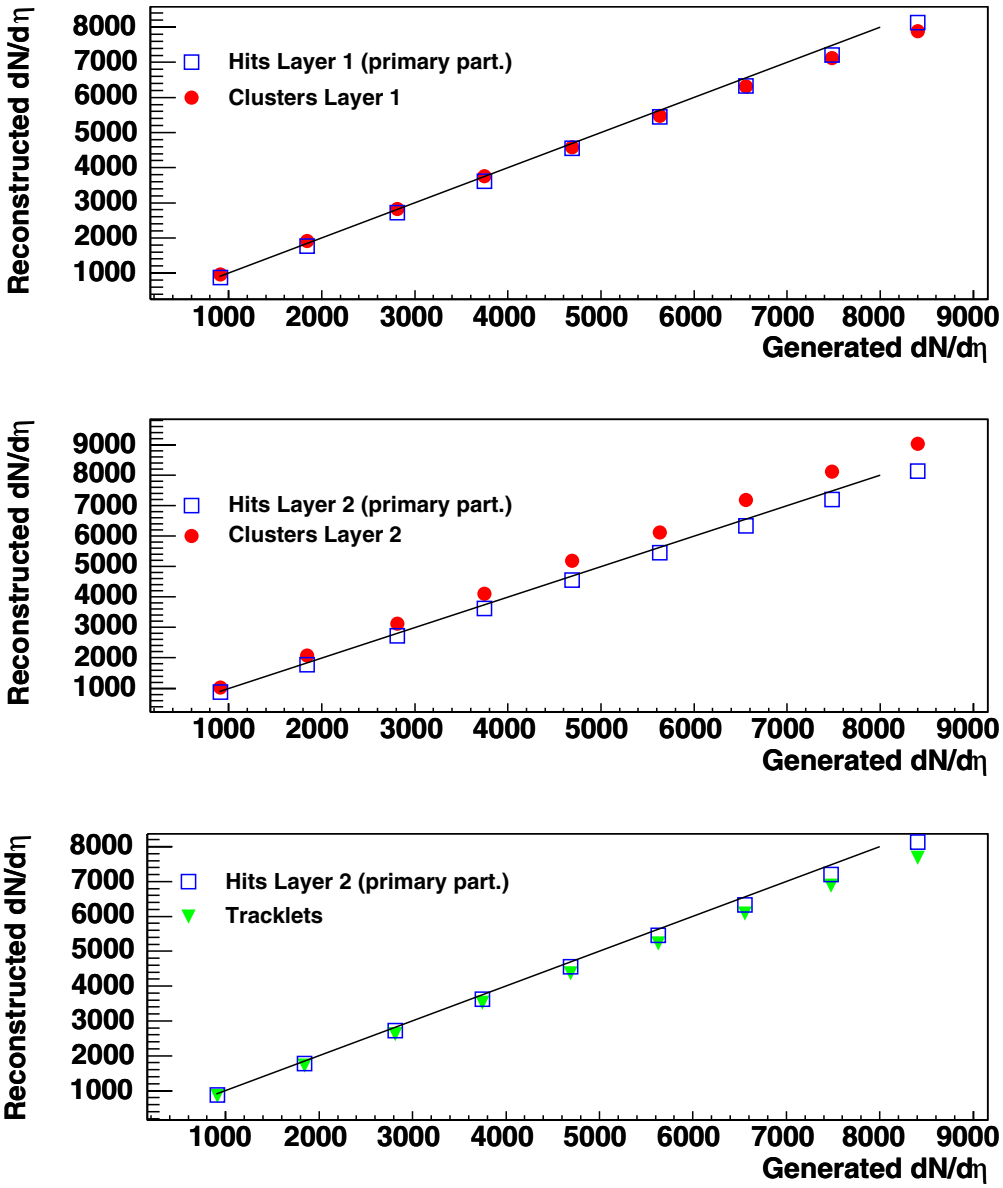


**Figure 1.** Number of hits and clusters for layer 1 (top) and 2 (center) and number of tracklets (bottom) in the central unit of $\eta$ as a function of the generated multiplicity. The straight line corresponds to the diagonal. The longitudinal vertex position is fixed to zero.

At very low multiplicity fluctuations become dominant, as shown in figure 3 where on the left side the reconstructed $dN/d\eta$ is shown as a function of the generated $dN/d\eta$, for each method. Two hundred events were generated for each multiplicity bin, and the distribution of the difference between reconstructed and generated $dN/d\eta$ was fitted by a Gaussian. The resulting $\sigma$ parameter is plotted as error bar on the same plot. The corresponding relative error ($\sigma/dN/d\eta$) is shown in the same figure (right side). It can be seen that a very low $dN/d\eta$ ($\simeq$ 10) can be measured within a 10% relative error.

The previous analysis was performed under the condition of no magnetic field. In figure 4

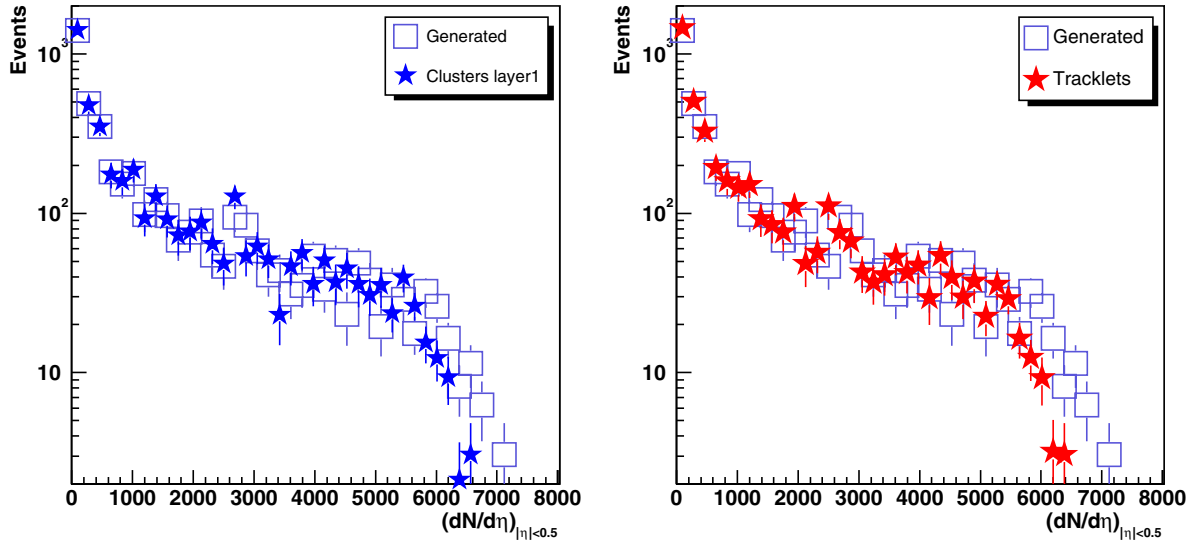


**Figure 2.** Generated and reconstructed multiplicity distribution. A mimum bias sample of about 1000 HIJING events is used.

the measured multiplicity is reported as a function of the magnetic field intensity. The field values are those foreseen to be used in the ALICE experiment (0.2, 0.4 and 0.5 Tesla). It can be seen that the number of clusters in the first layer is insensitive to the field, whereas the number of clusters in the second layer and therefore the number of tracklets is slowly decreasing with increasing field strength. This is mainly due to the tracks of very low momentum which are unable to hit the second layer.

For tracklets two different cuts on the fiducial window are used. It can be seen that in presence of magnetic field the efficiency strongly depends on the size of the fiducial window.

*2.4. $dN/d\eta$ reconstruction*

An example of $dN/d\eta$ reconstruction is reported in figure 5 for high multiplicity ($dN/d\eta$=6000) and $z_v = 0$. The full line corresponds in both plots to the generated $\eta$ distribution. In the upper picture the distributions obtained with hits (squares) and with clusters (points) both in the first layer are shown. Three "holes" are visible at $\eta$ =-1.35, $\eta$ =0 and $\eta$ =1.35, corresponding to the three geometrical junctions of the ladders. The two external points correspond to the geometrical limit of the layer. A good agreement between the original and the reconstructed distributions is obtained.

A good agreement is also obtained using the tracklets (bottom picture, triangles). The holes in this case appear also at the values $\eta$ =-0.8,$\eta$ = 0 and $\eta$ =0.8, corresponding to the junctions of the ladders of the second layer. The distribution reconstructed with the clusters in layer 2 is also shown for comparison (points). Here a clear overestimation can be seen, as expected.

The resolution on the determination of the single track pseudorapidity can be seen in figure 6, where a distribution track by track of the differences between generated and reconstructed $\eta$ is shown. A Gaussian fit gives a resolution $\sigma$=0.002.

An important aspect is the correlation between the multiplicity and the number of participants, and their ratio, which is connected with the fraction of soft and hard processes which are responsable for the particle production. The number of participants, $N_{part}$, will be measured in ALICE by the zero degree calorimeter (ZDC) [7]. The ratio $dN/d\eta/0.5 \cdot N_{part}$ as a function of $N_{part}$ is shown in figure 7, for the reconstructed (top) and the generated events

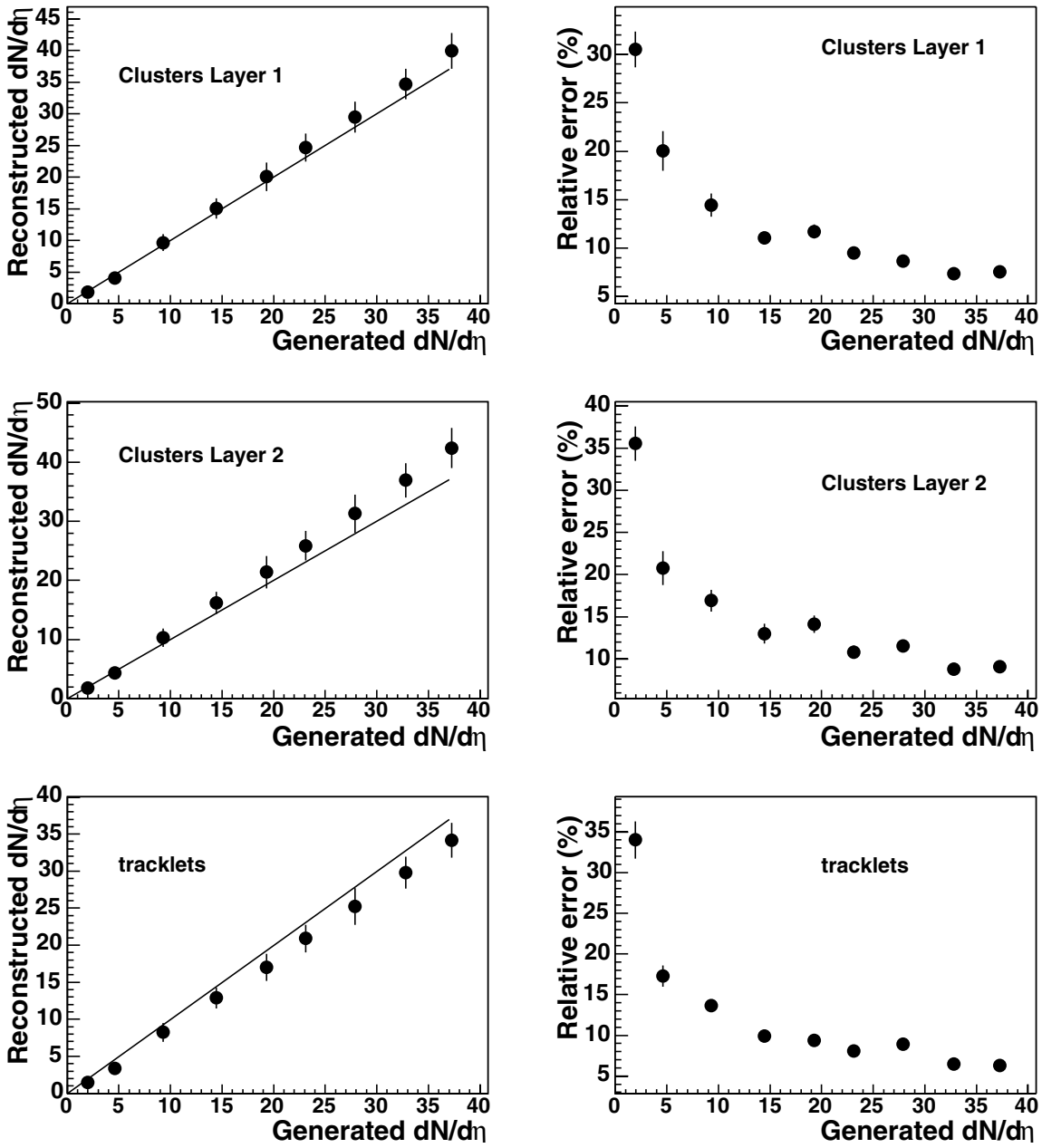


**Figure 3.** Spread of the reconstructed multiplicity ($dN/d\eta$) as a function of the generated $dN/d\eta$ (left), and relative error as a function of $dN/d\eta$ (right).

(bottom). The points are fitted with the expression (Kharzeev-Nardi approach [8]):

$$dN/d\eta/0.5 \cdot N_{part} = (1-x)n_{pp} + xn_{pp}\frac{N_{coll}}{0.5 \cdot N_{part}}$$

where $n_{pp}$ is the multiplicity measured in the p-p collisions. The number of collisions $N_{coll}$ has been determined from $N_{part}$ in the frame of the Glauber model, so $x$ is the only free parameter of the fit. The value of $x$ for the reconstructed data are $x$=0.60±0.03 (clusters) and $x$=0.57±0.03

(tracklets) in good agreement with the result of the fit to the generated ratio, which yields $x$=0.61±0.03.

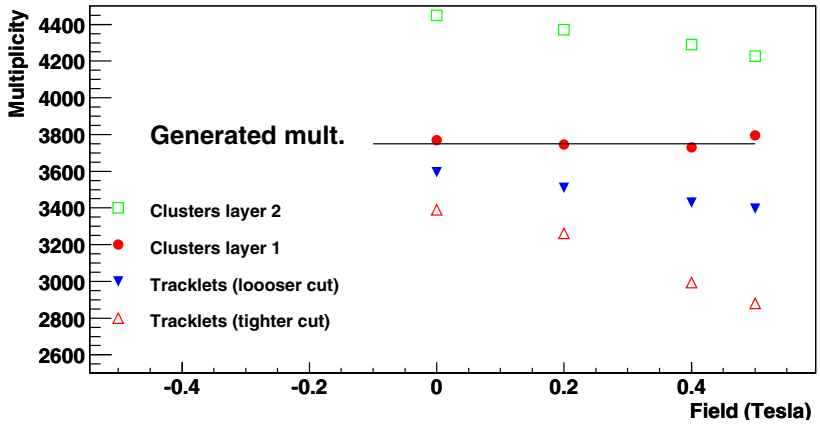


**Figure 4.** Reconstructed multiplicity as a function of the magnetic field intensity. For tracklets two different cuts on the fiducial window are considered.

## 3. Multiplicity and $dN/d\eta$ distribution in the forward region

The study of the charged particle distribution over a wide $\eta$ range plays an important role in the event characterization. In particular, the forward region is essential in order to really constrain the models and to investigate effects connected with the fragmentation of the projectile and the target.

The measurement of the charged particle multiplicity and the reconstruction of the pseudorapidity distribution in the forward and backward regions of $\eta$ will be performed by a dedicated detector, the Forward Multiplicity Detector (FMD) [1]. It consists of three crowns of silicon ring detectors, covering the pseudorapidity ranges $-5.1 < \eta < -1.7$ and $1.7 < \eta < 3.4$. In the present layout 512 rings and 20 sectors are foreseen for the inner crowns, while the outer crown will be divided into 256 rings and 20 sectors. Unfortunatley, even with this granularity it turns out that the occupancy in the detector for high multiplicity events will be of the order of one or even larger. In this case it will not be possible to determine the multiplicity by simply counting the pads which have fired, due to the large contribution of hits from more than one incident particle. A method based on the counting of empty pads has been developed for this case. The simulation show in fact that with the present geometry and granularity of the FMD, and for a mean occupancy per pad ranging from 0.4 to 2.2, there is a statistically significant number of empty pads when one consider 0.1 units wide pseudorapidity bins. Therefore, using the Poisson statistics, the average occupancy $\lambda$ can be determind as $\lambda = -\ln P(0)$, where the probability $P(0) = N_e/N_{tot}$ is the ratio between the number of empty pads $N_e$ to the total number of pads $N_{tot}$ in a certain $\Delta\eta$ interval. Then, the total multiplicity $n$ can be simply calculated as $n = \lambda \cdot N_{tot}$. The accuracy of this method is better than 3%.

In order to determine the real primary multiplicity a background subtraction must be performed. The simulation shows [9] that most of the background comes from the the ITS detector structure and from the beam pipe. The correction coefficients as a function of $\eta$ have been determined using a simulation based on a sample of 200 HIJING events. This coefficients can have a dependence on the pseudorapidity distribution used in the generation, so in principle they can be determined by iterations.

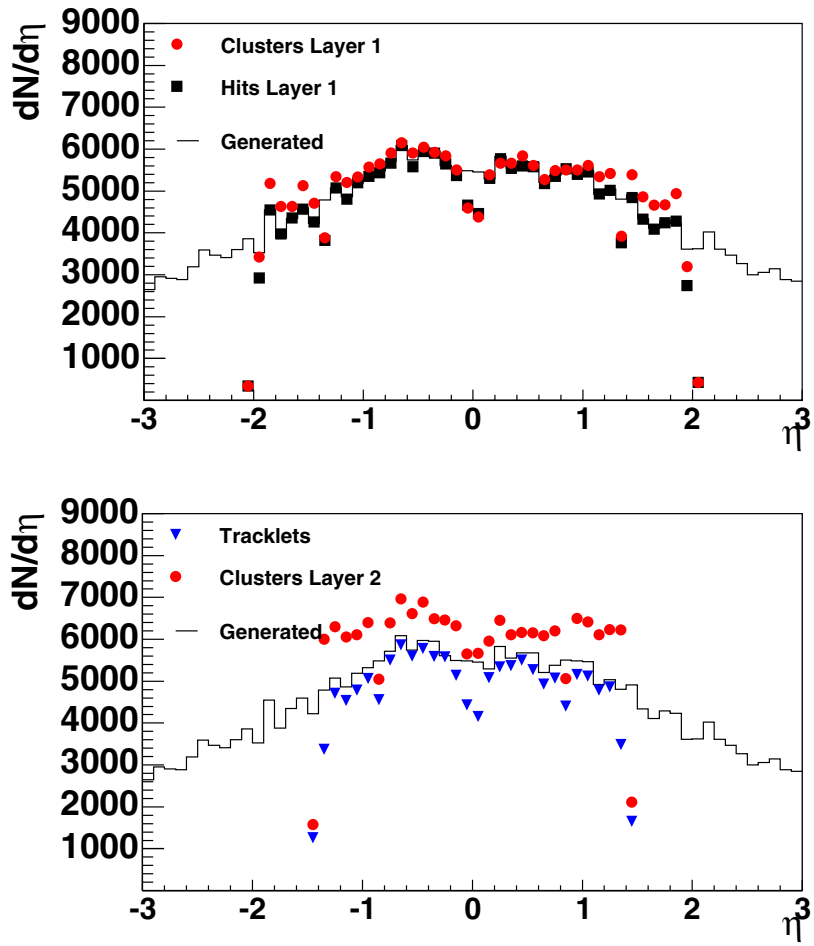


**Figure 5.** Generated and reconstructed $\eta$ distribution.

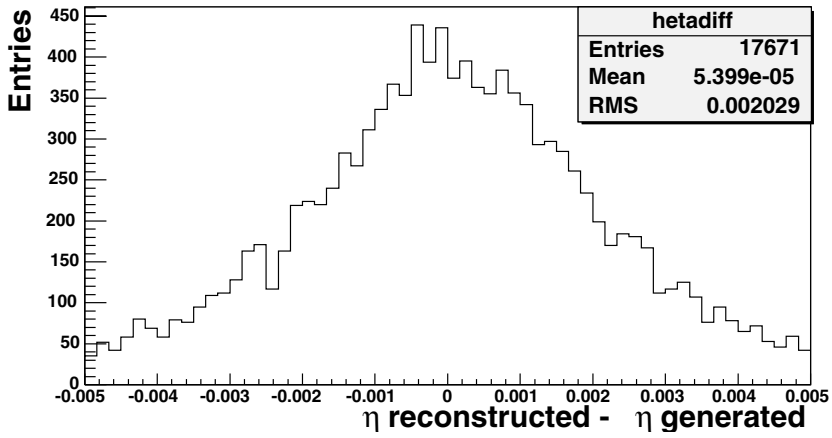


**Figure 6.** Distribution of the differences between generated and reconstructed $\eta$.

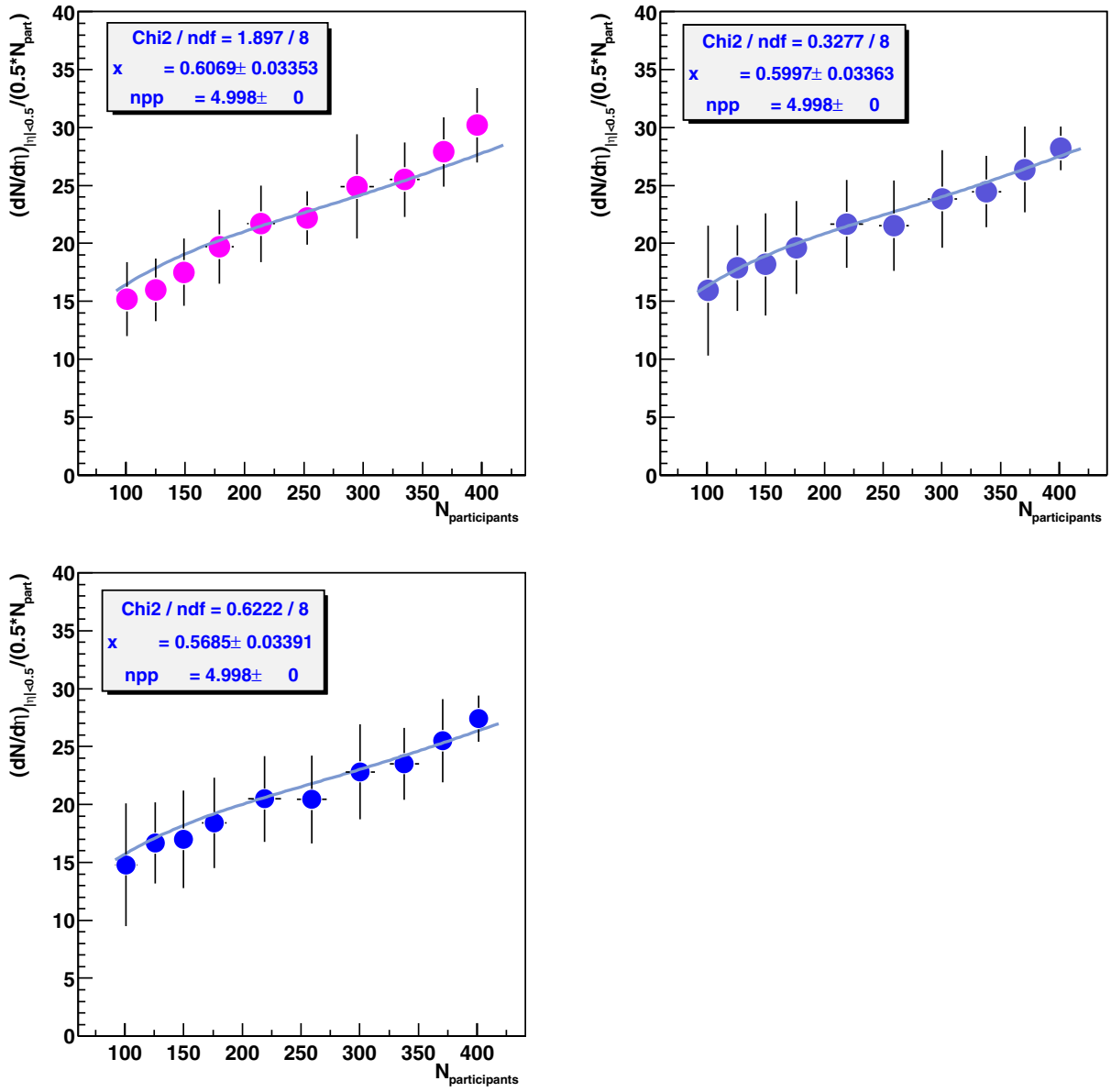


**Figure 7.** Ratio of the multiplicity to one half of the number of participant $N_{participants}$ as a function of $N_{participants}$. Top left: reconstruction with the clusters in layer 1; top right: reconstruction with the tracklets; bottom: generated. The results of the fit are also shown (see text).

The corrected multiplicities as a function of the generated ones are shown in figure 8 for some specific pseudorapidities (left side), together with the relative errors (right side). The triangles and the dots correspond to the relative errors on the total multiplicity (primary and background) and on the primary one respectively.

An example of a reconstructed pseudorapidity distribution is shown in figure 9. It corresponds to a set of 80 HIJING central events ($dN/d\eta = 6000$ at $\eta = 0$).

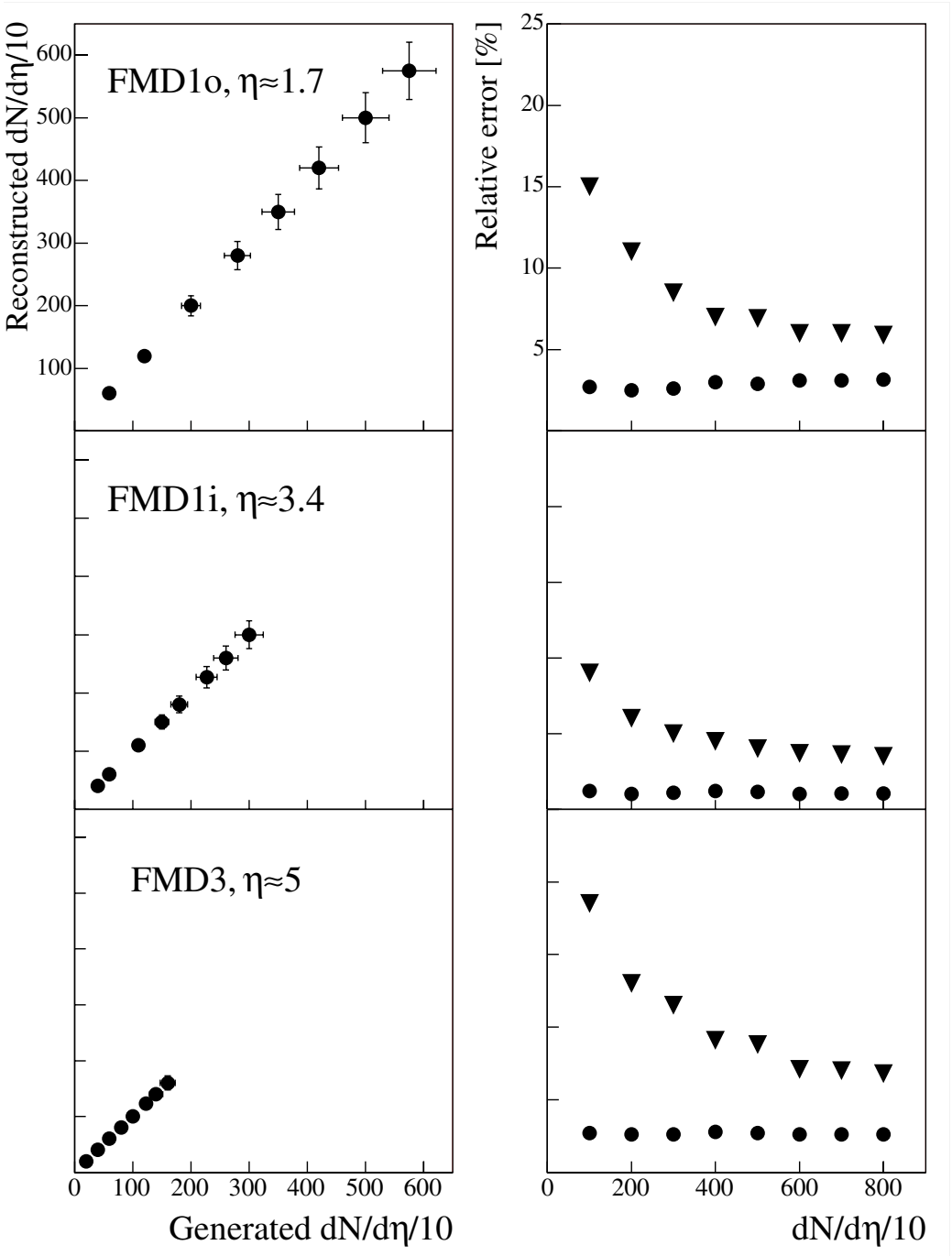


**Figure 8.** Reconstruction of the multiplicity with the FMD in selected $\eta$ ranges, and relative error. The larger errors correspond to the reconstruction of the total (primary plus secondary) multiplicity, the lower to the primary multiplicity.

## 4. Conclusions

We have shown that the ALICE experiment will be able to measure the multiplicity of the charged tracks over a wide range of pseudorapidity (almost 10 $\eta$-units, with an accuracy of 7% for a single event with a bin width of 0.1 $\eta$-units. For the central region, both the presented

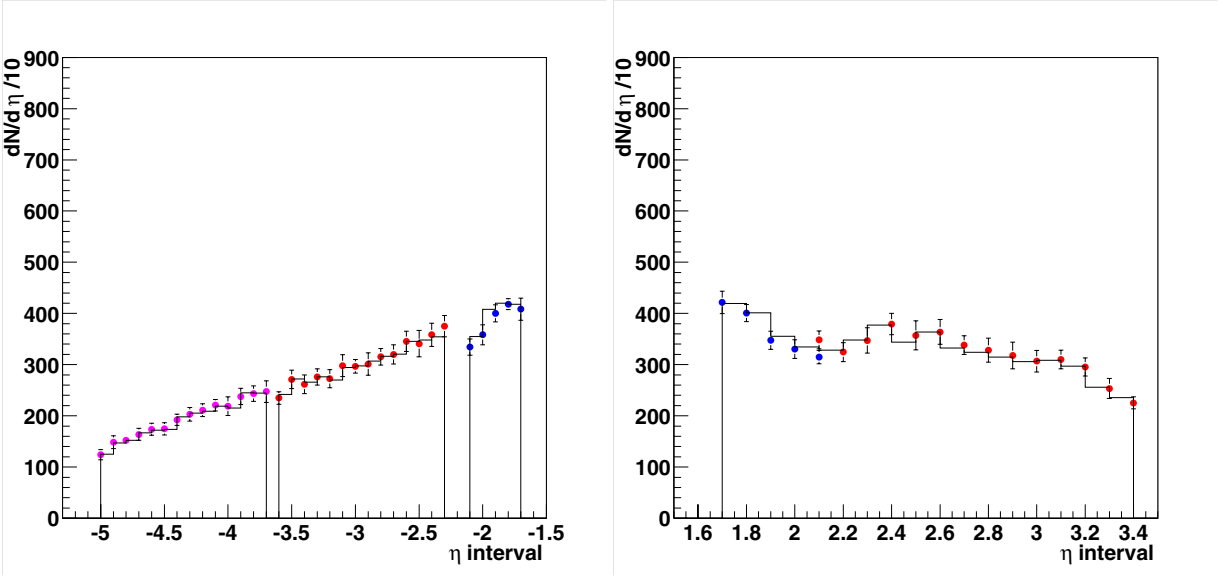


**Figure 9.** Reconstruction of the $\eta$ distribution with the FMD.

methods give a good estimate of the event multiplicity. In this range the statistical errors allow to measure event multiplicities as low as $dN/d\eta$=10-15 within 10% relative error; the resolution on the determination of the single track pseudorapidity is about 0.002.

## References

[1] ALICE Physics Performance Report Vol. I ALICE Collaboration 2004 *J. Phys. G: Nucl. Part. Phys.* **30** 1517-1763
[2] Letessier J, Tounsi A, Heinz U, Sollfrank J and Rafelski J 1995 *Phys. Rev.* D **51** 3408
[3] Bjorken J D 1983 *Phys. Rev.* D **27** 140
[4] Badalà A, Barbera R, Lo Re G, Palmeri A, Pulvirenti A, Pappalardo G S, Riggi F for the ALICE Collaboration 2002 *Nucl. Instrum. Methods Phys. Res.* A **485** 100
[5] ALICE Collaboration 1999 ALICE TDR 4 CERN/LHCC 99-12
[6] Caliandro R, Di Napoli R, Fini R A and Virgili T 2001 ALICE 2001-05 Internal Note/SIM
Caliandro R, Fini R A and Virgili T 2002 ALICE 2002-043 Internal Note/SIM
[7] ALICE Collaboration 1999 "Zero-Degree Calorimeter Technical Design Report" CERN/LHCC 99-5
[8] Kharzeev D E and Nardi M 2001 *Phys. Lett* B **507** 121
[9] ALICE Physics Performance Report Vol. II, ALICE Collaboration, to be published